# Supplementary Methods

## Molecular cloning

All Ace fusion proteins (including mOrange2, mRuby3, mRuby4, Halotag, and SNAP-tag) were generated by fusing protein tags to the C-terminus of Ace in FCK vector[1], using Gibson assembly protocol following manufacturer's instructions[2]. Ace mutants were generated by QuikChange following the manufacturer's protocol, using Phanta Max Super-Fidelity DNA Polymerase (Vazyme). Plasmids were purified by Midiprep Kit following the manufacturer's protocol (Tiangen, China).

To construct plasmids encoding mRuby4 fusions, the following plasmids as described earlier[3] were digested by the corresponding restriction enzymes and purified: pCyOFP1-14aa-RhoB, pCyOFP1-10aa-H2B, pCyOFP1-18aa-tubulin and pCyOFP1-5aa-CAAX by a 5' AgeI and a 3' BglII; pCx43-7aa-CyOFP1, pGalT-7aa-CyOFP1, and pCalnexin-14aa-CyOFP1 by a 5' AleI and a 3' NotI. mRuby4 cDNA was amplified by PCR, then purified and ligated into these digested vector backbones containing fragments encoding various organelle-targeting domains using In-Fusion HD Cloning Kit (Clontech). Domains for fusion proteins were derived from the following sources: human RhoB, NM_004040.2; human H2B, NM_021058.3; human α-tubulin, NM_006082; rat connexin-43, NM_012326.2; human galactosyltransferase 1, NM_001497.3; c-Ha-Ras, NM_001130442.1; human Calnexin, NM_001746.3. Full sequences of plasmids are available upon request.

## Characterization of voltage response in HEK293T cells

Human embryonic kidney (HEK) 293T cells were cultured in Dulbecco's Modified Eagle's medium (DMEM) (Thermo Fisher Scientific) supplemented with 10% v/v fetal bovine serum (FBS) (Gibco). Cells were transfected with Lipofectamine 2000 (Invitrogen) at 70%-90% confluent following manufacturer's protocol. 24 hours after transfection, cells were re-plated to glass coverslip (Tian Nuo Tian Cheng) pre-coated with 1:50 matrigel for 30 min (BD).

To control membrane voltage, whole-cell voltage clamp was applied to transfected HEK293T cells, as previously described[1]. Specifically, the patch clamp was controlled with Axopatch 200B amplifier (Axon Instruments) and positioned by a Sutter MP285 micro-manipulator. The borosilicate glass electrode was filled with intracellular buffer (IC buffer) with the following formulation: 125 mM potassium gluconate, 8 mM NaCl, 0.6 mM $MgCl_2$, 0.1 mM $CaCl_2$, 1 mM EGTA, 10 mM HEPES, 4 mM Mg-ATP, 0.4 mM Na-GTP (pH 7.3). The osmolarity was adjusted to 295 mOsm/kg with 1 M sucrose solution. Tip resistance was measured to be in the range of 2.5 to 5 MΩ. Patch clamp voltage command and data collection were controlled with a National Instruments PCIe-6353 data acquisition (DAQ) board and homebuilt LabView software (v15.0,

National Instruments). The electrical signal was filtered with an internal Bessel filter (bandwidth 5 kHz) and digitized at 9682 Hz.

To measure voltage sensitivity, a triangle wave was applied through voltage clamp. Voltage command varied linearly between -100 mV and 50 mV with a period of 6 seconds. Cells were simultaneously illuminated with excitation light and imaged on a homebuilt fluorescence microscope (Nikon-TiE equipped with 40x NA1.3 oil immersion objective and Coherent OBIS laser lines). 488 nm (6.0 W/cm$^2$) was used for imaging mNeonGreen, 532 nm (3.5 W/cm$^2$) for mOrange2, and 561 nm (5.0 W/cm$^2$) for mRuby3/4 and TMR dye. Movies were acquired at 10 Hz frame rate, at 2-by-2 binning on a scientific CMOS camera (sCMOS, Hamamatsu ORCA-Flash 4.0 v2). To measure response kinetics, a square wave was applied that varied between -70 mV and 30 mV. The same image acquisition protocol was applied as described above, except for a faster frame rate (camera frame rate of 1058 Hz, which gives an exposure time of 0.9452 ms). Data analysis was performed with MATLAB (version 2014B, MathWorks).

**Voltage imaging in cultured neurons**

Rat hippocampal neurons were dissected from P0 rat pups and plated on pre-coated glass coverslips and maintained in Neurobasal medium (Thermo Fisher Scientific) supplemented with 2% v/v B27 (Gibco), 1% v/v GlutaMAX™ (Thermo Fisher Scientific) and 1% v/v Penicillin-Streptomycin (Thermo Fisher Scientific). Glass coverslips were pre-treated with poly-D-lysine (10 μg/mL for 24 hours, Sigma), followed by laminin (20μg/mL for 24 hours, Thermo Fisher Scientific) in a 24-well plate. Neurons were transfected with Lipofectamine 2000 (Invitrogen) on DIV (days *in vitro*) 8-9, with slight modification from manufacturer's protocol: Neurobasal medium was used to dilute plasmids in place of Opti-MEM, and neurons were only briefly incubated with the transfection mixture, typically for 10 minutes. We noticed poor cell health with prolonged incubation.

Imaging was typically performed on DIV12-14. To stimulate neuronal action potentials (APs), current pulses were injected into neurons via whole-cell current clamp. Patch clamp operation was similar as described above, except that it operated in current clamp mode. A typical stimulation protocol injected 80 pulsed currents at 4 Hz, each lasting 4 ms with an amplitude of 400 pA. Alternatively, weaker currents (typically 260 -285pA) were applied for a longer period (516 ms) to stimulate firing of AP spike trains. Command voltage for the patch clamp amplifier and data collection were controlled with the DAQ acquisition card described in the previous section. For all-optical electrophysiology, neurons expressing CheRiff and Ace(D81S)-mOrange2/mRuby4 were illuminated with 561 nm excitation light (5.0 W/cm$^2$) and stimulated with 405 nm laser pulses (2 ms duration at 1.4 W/cm$^2$, repeated at 5 Hz).

Neurons with medium expression levels were selected for analysis. We noticed that neurons

with extremely high levels of GEVI expression tended to have abnormal morphology. Neurons with low AP amplitudes (<70 mV) were excluded from our analysis. Image series were acquired at a camera frame rate of 484 Hz. To quantify fluorescence response, ROIs around the soma were drawn manually and all pixels in the ROI were used to calculate the $\Delta F/F_0$. No pixels were excluded from the analysis.

**Halotag/SNAP-tag labeling**

For HEK293T cells, 30 hours after transfection, cells were incubated with complete medium containing cell-permeant dye, either 5 μM TMR-Halotag ligand (Promega) or 3 μM TMR-SNAP-tag ligands (New England BioLabs), for 15 minutes at 37℃, 5% $CO_2$. Cells were washed five times with fresh complete medium to remove unbound ligand. Rat hippocampal neurons expressing Ace-Halotag fusions were typically labeled 3 days post-transfection, using 30-300 nM dye concentration for 5-30 min at 37℃ (Figure S20). Complete Neurobasal medium including B-27 Supplement and GlutaMax was used as the labeling buffer for neurons, instead of DMEM/FBS.

**mRuby4 mutagenesis and library screening**

We started with mRuby3[30]. A tandem fusion protein of green mNeonGreen and red mRuby3 with high FRET was used as an initial template for screening brighter and more photostable mRuby3 variants. It has been shown that residues at the outer barrel surface, the inner barrel surface and the loop are known to affect FP's brightness and photostability[6]. We first attempted to improve the brightness by repacking residues near the chromophore and stabilizing the long loop between β-strands 9 and 10. However, variants brighter than mRuby3 were not found from these two libraries. We then introduced mutations into the outer barrel to optimize folding or maturation. In each round, bacterial colonies were screened for high fluorescence followed by photostability examination using an inverted microscope, and the bright mutant with high photostability was used as a template for the subsequent round. After 3 rounds of screening, we identified a bright variant containing 12 substitutions relative to its parent mRuby3 (N8E, R10P, E16T, S18T, Q23Y, E111Q, E114V, V116I, V124E, N173S, T177E, R179K) (Figure S21). The resultant mutant, called mRuby4, has excitation and emission maxima at 558 and 592 nm (Figure S22), respectively, identical to mRuby3. Two rounds of random mutagenesis by error-prone PCR did not generate any better variants.

Mutations for specific residues were introduced by overlap-extension PCR and random mutagenesis was performed by error-prone PCR using Taq DNA polymerase (Tiangen, China). Mutants were expressed and screened in constitutively active bacterial expression vector pNCS (Allele Biotech). Plasmids were transformed into chemically competent Stellar *E. coli*, and colonies were grown on SOB agar plates at 34°C for 16-20 hours. The number of colonies screened was 10-

fold the expected library diversity to ensure full coverage for each round of mutagenesis. Bright colonies exhibiting a larger emission ratio (FRET/green) than that of mNeonGreen-mRuby3 were screened with a home-made bacterial screening system and then examined for photostability in bacteria using an IX83 microscope.

### *In vitro* fluorescent protein characterization

We characterized mRuby4 for monomericity, brightness, chromophore maturation, pH stability *in vitro* and in bacteria. mRuby4 was monomeric at high concentration of 10 mg/mL (Figure S23), consistent with the fact that all mutations are not in the dimerization interface. The peak extinction coefficient is 132 $mM^{-1}$ $cm^{-1}$, and the quantum yield is 0.45, resulting in a calculated molecular brightness 3.5% greater than that of mRuby3. Furthermore, mRuby4 exhibited 28% higher final maturation efficiency than mRuby3 (Table S1). However, when fused to mNeonGreen, mRuby4 exhibited ~70% higher fluorescence emission peak ratio (red/green) than mRuby3 (Figure S24), which was larger than expected from molecular brightness (70% vs 3.5%), suggesting its more complete maturation. The fluorescence of mRuby4 was comparably resistant to acid pH compared to mRuby3, with a pKa of 4.8 (Figure S25 and Table S1).

Fluorescent proteins with N-terminal hexahistidine tags were purified with HisPur Cobalt Resin (Pierce) and desalted into phosphate buffered saline (PBS, pH = 7.2) using Econo-Pac 10DG desalting columns (Bio-Rad). The monomericity of mRuby4 at high concentration (10 mg/mL) was verified by high performance liquid chromatography using LC-20AD (Shimadzu) equipped with a UV/Visible dual wavelength detector (SPD-20A, Shimadzu) and a Superdex 200 10/300 GL column (GE Bioscience). Excitation and emission spectra were measured with an Infinite M1000PRO microplate reader (Tecan). Extinction coefficients were calculated using previously described base-denaturation method[4]. Quantum yields were determined using mRuby3 as a standard (quantum yield, QY = 0.45). pH titrations were performed using a series of buffers containing 50 mM $Na_2HPO_4$, 50 mM sodium acetate, and 50 mM glycine, with a pH range between 2 and 10.

### Characterization of mRuby4 in mammalian cells

We further assessed mRuby4 performance in mammalian cells. First, mRuby4 had 18% better photostability than mRuby3 under wide-field illumination in living cells (Figure S26 and Table S1), and exhibited negligible photochromic behavior (Figure S18). In cultured rat hippocampal neurons, Ace(D81S)-mRuby4 is 25% more photostable than Ace(D81S)-mRuby3 (VARNAM) when illuminated with 561 nm laser ($t_{1/2}$ = 475 ± 23 s vs. 381 ± 9 s, mean ± s.e.m., n = 3). Next, we confirmed that a variety of mRuby4 fusions to subcellular targeting sequences including histone H2B localized correctly in HEK293T cells (Figure S27). Lastly, we compared mRuby4 to mRuby3

for brightness by co-expressing mRubyX (mRuby3 or mRuby4) and cyan FP mTurquoise2 in HEK293T and CHO cells. mRubyX and mTurquoise2 were separated by a self-cleaving P2A peptide, and mTurquoise2 was used to normalize for mRNA differences between two samples. Consistent with the results in bacteria, mRuby4 was ~90% brighter than mRuby3 when expressed in mammalian cells (compared to 70% in bacteria) (Figure S28 and S29). Overall, these results indicate that mRuby4 is brighter, more photostable and folds better than mRuby3.

Cells were maintained in high-glucose Dulbecco's Modified Eagle Medium (DMEM, HyClone) supplemented with 5% fetal bovine serum (BI), 100 U/mL penicillin and 100 μg/mL streptomycin (HyClone) at 37 °C with 5% CO2. Cells were transfected at 80-90% confluence with Lipofectamine 2000 (Life Technologies) in Opti-MEM (Gibco). For expressing mRuby4 fusion proteins, HEK293T cells were transfected in 24-well plates, and the medium was refreshed 6-8 hours after transfection. 24 hours later, cells were split into 35-mm glass-bottom dishes (D35-20-1.5-N, MatTek) and cultured for another 24 hours before imaging in Live Cell Imaging Solution (Life Technologies). Fluorescence images (1024 × 1024 pixels) were acquired under 561 nm laser excitation on a Nikon A1 confocal microscope with a 60× oil-immersion (NA 1.4) objective (Nikon). Image processing was performed with ImageJ (https://imagej.nih.gov/ij/).

For photostability measurements, HEK293T cells expressing the mRuby4-H2B fusion were transfected and replated to MatTek dishes as described above and imaged 48-hr post-transfection. Cells were immersed in Live Cell Imaging Solution (Life Technologies) and imaged using an Olympus IX83 inverted microscope with a silicone immersion 40 × 1.25-NA UPLSAPO objective, a 130-W U-HGLGPS metal halide lamp (Olympus) at 100% neutral density passed through a 540/25 nm excitation filter (Chroma). The power at the back focal plane of the objective was 13.9 W/cm2. Fluorescence images were acquired every 1 s under continuous illumination using an optiMOS camera (QImaging). The photobleaching data was corrected to the transmission spectra of the excitation and emission filters, the absorption spectra and of mRuby variants, and molecular brightness (QY × EC).

For brightness comparison, HEK293T and CHO cells were transfected in 6-well plates and the medium was refreshed 8 hours after transfection as above, and cultured for another 24 and 48 hours before experiments were performed. Comparison of mRuby3 and mRuby4 brightness in mammalian cells was made using mTurquoise2 as an expression level reference. Fusions were expressed in cells using Lipofectamine 2000 (Life Technologies). At 24 and 48 hours post-transfection, cells were transferred to a transparent-bottom 96-well plate and fluorescence spectra or intensity under a given wavelength were obtained on an Infinite M1000PRO microplate reader (Tecan). The excitation and emission monochromators settings are as follows (FP-ex-em): mTurquoise2-434/5 nm-474/5 nm and mRuby3/4-550/10 nm-570~670 nm. Relative brightness was calculated from integrated mRuby variants emission divided by peak mTurquoise2 emission.

Student’s t-test was used to determine the differences between mRuby3 and mRuby4. Statistical analysis was performed in Excel (Microsoft).

## Supplementary Figures

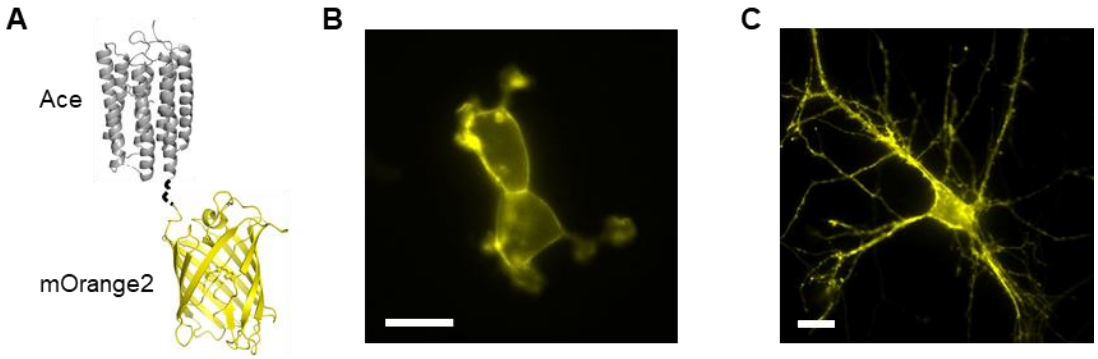


**Figure S1. Expression of Ace-SG-mOrange2 in cultured rat hippocampal neurons.** (A) Model of Ace-SG-mOrange2. (B-C) Fluorescence images of HEK293T cells (B) and neurons (C) expressing Ace-SG-mOrange2. Scale bar = 20 μm.

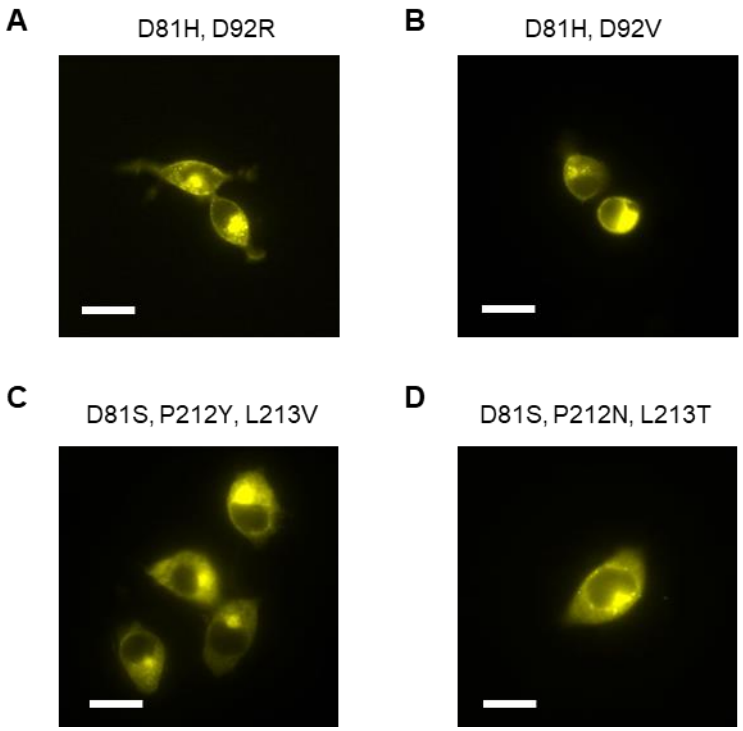


**Figure S2. Expression and membrane trafficking of Ace-SG-mOrange2 mutants in HEK293T cells.** Mutations in Ace are shown above each fluorescence image. Scale bar = 20 μm.

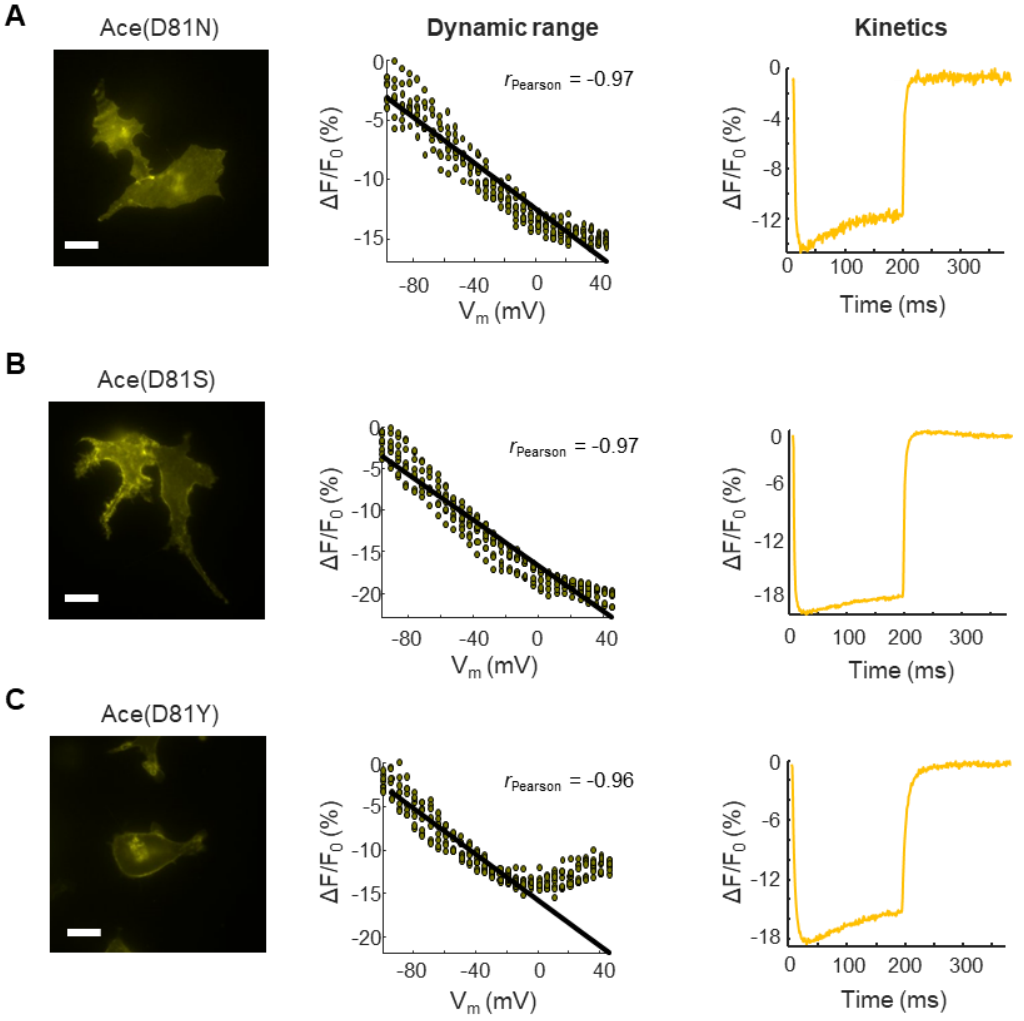


**Figure S3. Expression, dynamic ranges, and kinetics of Ace-SG-mOrange2 mutants in HEK293T cells.** Left: fluorescence images of mOrange2, with mutations of Ace indicated above each image. Middle: measurement of fluorescence response to voltage changes (F-V curve), with linear fit line displayed on top of the data points and Pearson's correlation coefficient listed on the right. For Ace(D81Y)-SG-mOrange2 (C), the linear fit was limited to the range between -100 mV and 0 mV. Right: fluorescence response to square wave voltage change. Scale bar = 20 μm.

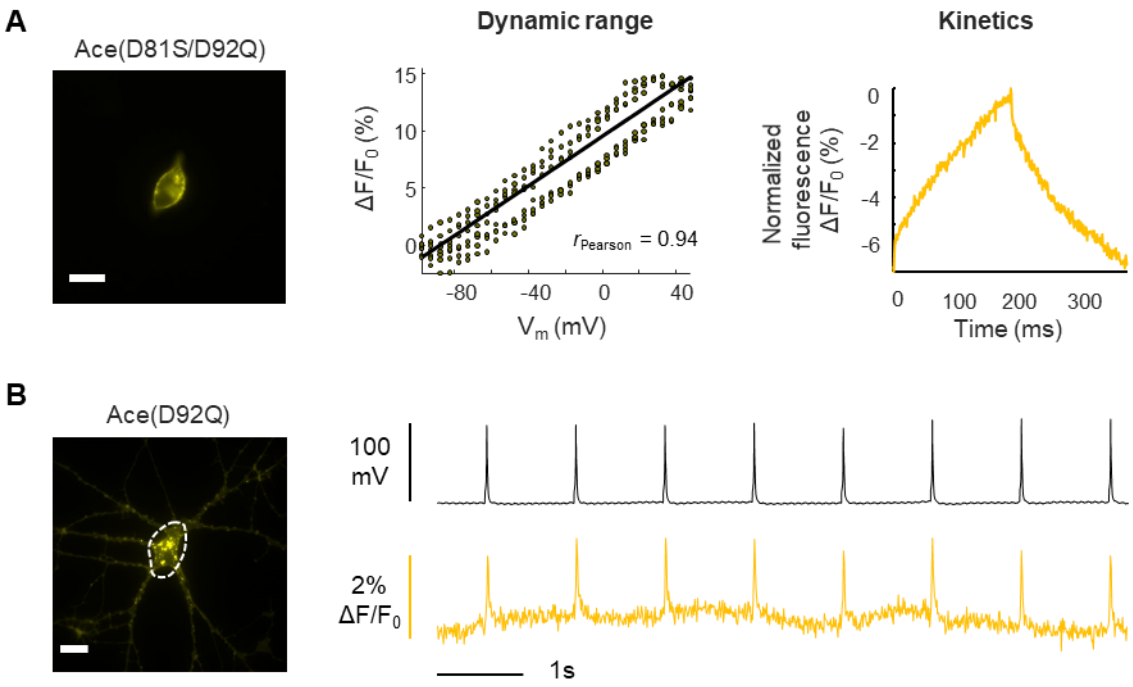


**Figure S4. Expression, dynamic range and kinetics of Ace(D92Q)-SG-mOrange2 mutants in HEK293T cells and neurons.** (A) Characterization in HEK293T cells. Left: fluorescence images of Ace(D81S/D92Q)-mOrange2. Middle: fluorescence response to membrane voltage changes (F-V curve), with a linear fit line displayed on top of the data points and Pearson's correlation coefficient. Right: fluorescence response kinetics. (B) Characterization in cultured rat hippocampal neurons. Left: fluorescence images of a neuron expressing Ace(D92Q)-SG-mOrange2. Right: fluorescence response of Ace(D92Q)-SG-mOrange2 to stimulated APs. Scale bar = 20 μm.

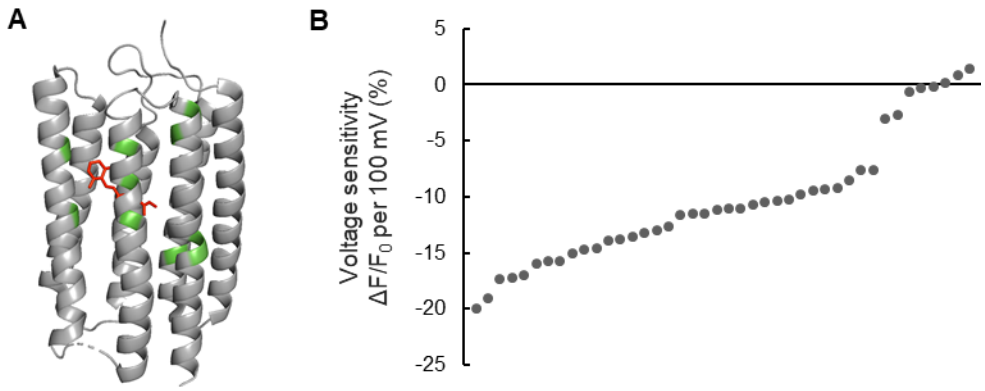


**Figure S5. Voltage sensitivity of point mutations surrounding the retinal chromophore.** (A) Ace structure showing retinal chromophore (red) and mutated sites (green), including residues involved in the proton transfer pathway (N45, D197, E199) and proximal to the retinal chromophore (F134, Q141, W178, Y181, W185, P212, L213). (B) Summary of voltage sensitivity screening of Ace-SG-mOrange2 mutants in HEK293T cells.

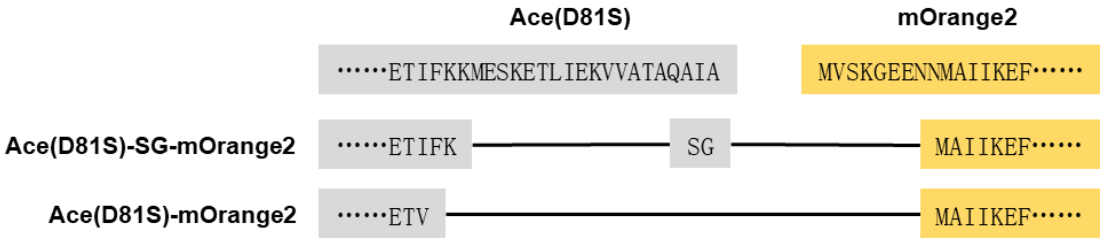


**Figure S6. Linker optimization to improve voltage sensitivity.**

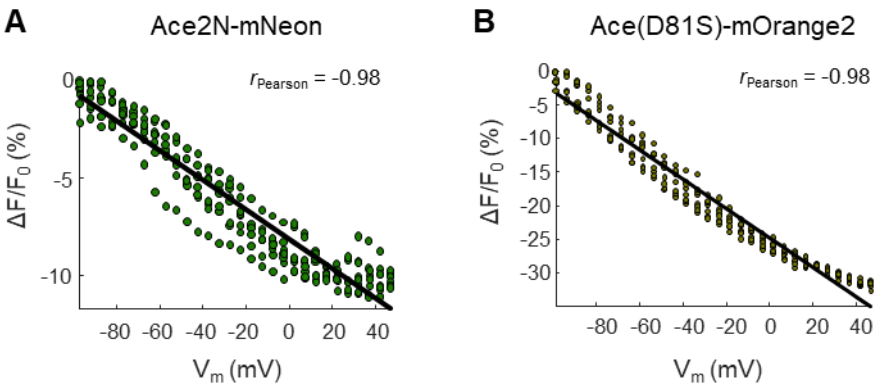


**Figure S7. Characterization of dynamic range in HEK293T cells.** Fluorescence response of Ace2N-mNeon (A) and Ace(D81S)-mOrange2 (B) to membrane voltage changes, with a linear fit line displayed on top of the data points and Pearson's correlation coefficient.

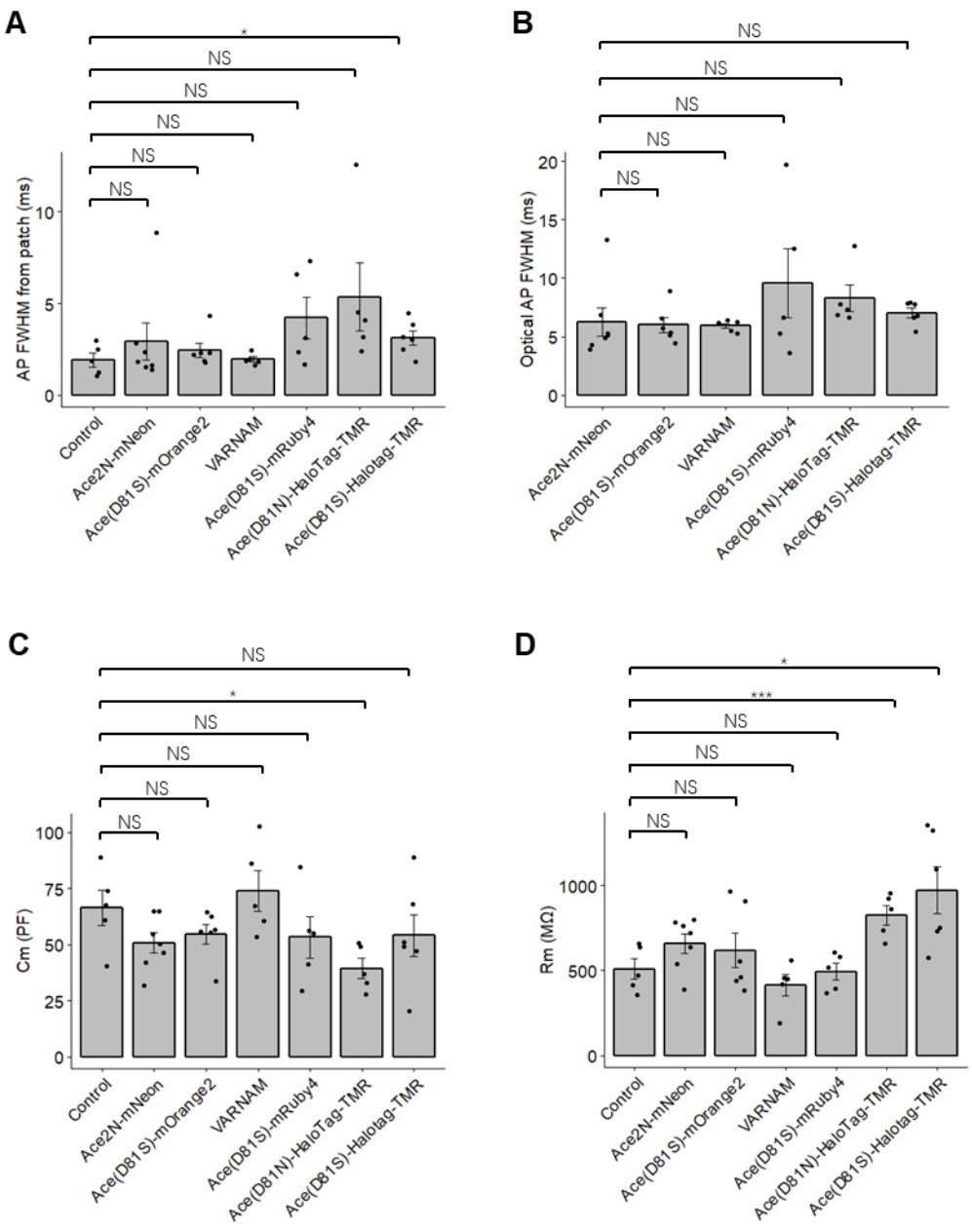


**Figure S8. Effects of GEVI expressions on the FWHM of stimulated action potentials and cellular electrophysiology.** (A) Full width at half maxima (FWHM) of optical recording of AP. (B) FWHM of electrical recording of AP. (C-D) Membrane capacitance (C) and membrane resistance (D) of neurons expressing GEVIs. NS: not significant ($p > 0.05$); * $p < 0.05$; *** $p < 0.001$. Data are presented as mean ± S.E.M. P-values between different groups were calculated using the Student t-test.

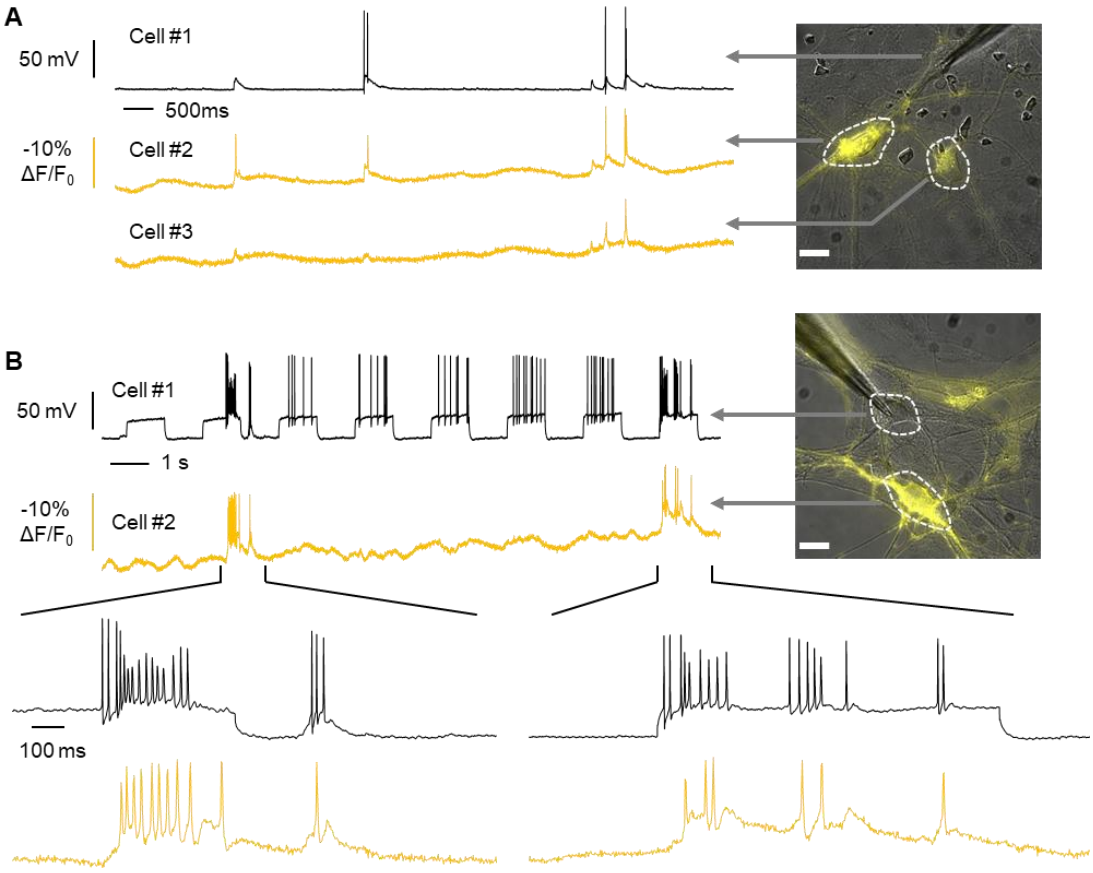


**Figure S9. Application of Ace(D81S)-mOrange2 to map functional connectivity.** (A) Spontaneous APs were recorded by patch clamp and Ace(D81S)-mOrange2 in three neighboring cells. (B) Stimulated AP bursts in one neuron were time-correlated with electrical activity in neighboring cells, as revealed by voltage imaging. Scale bar = 20 μm.

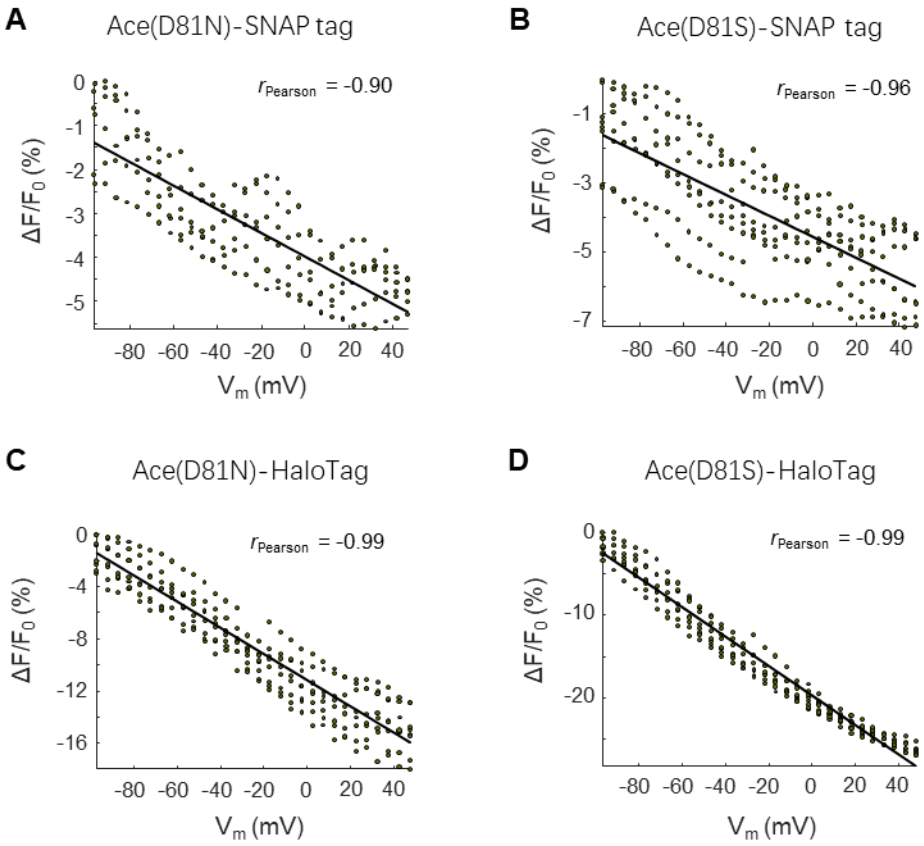


**Figure S10. F-V response curve for Ace(D81N/S)-Halotag/SNAP-tag variants.** A linear fit is shown as a straight line, with Pearson's correlation coefficients shown in the upper right corner of each panel. (A) Ace(D81N)-SNAP-tag, (B) Ace(D81S)-SNAP-tag, (C) Ace(D81N)-Halotag, (D) Ace(D81S)-Halotag.

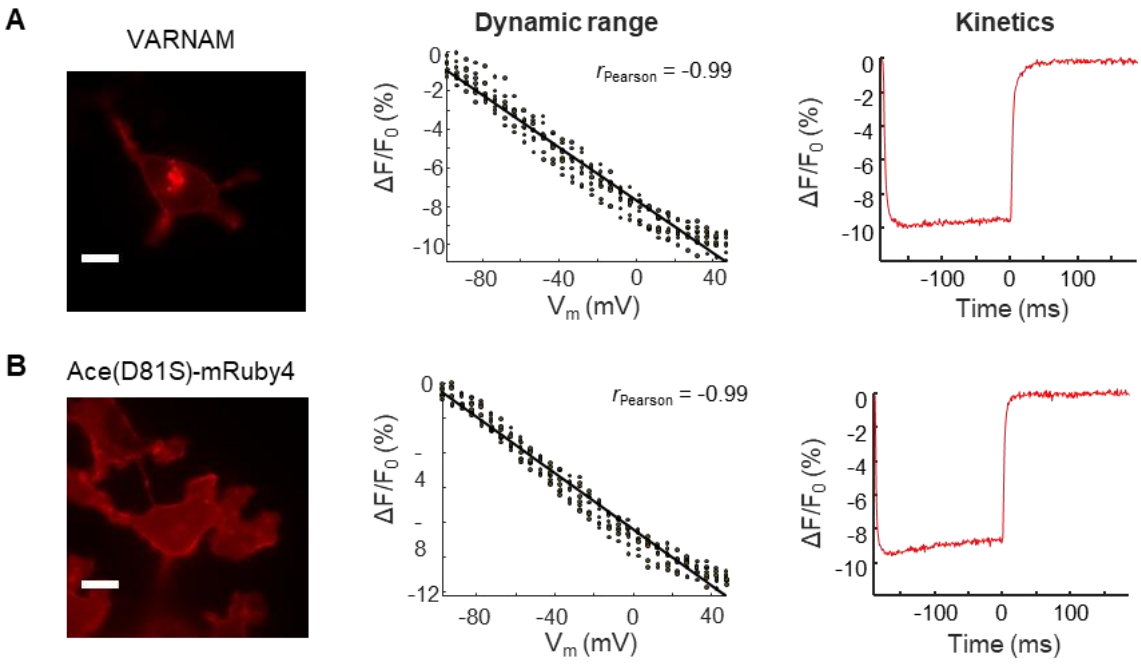


**Figure S11. Expression, dynamic ranges, and response kinetics of VARNAM and Ace(D81S)-mRuby4 in HEK293T cells**. Left: fluorescence images of VARNAM and Ace(D81S)-mRuby4. Middle: fluorescence response to membrane voltage changes (F-V curve), with a linear fit line displayed on top of the data points and Pearson's correlation coefficient. Right: fluorescence response kinetics. Scale bar = 20 μm.

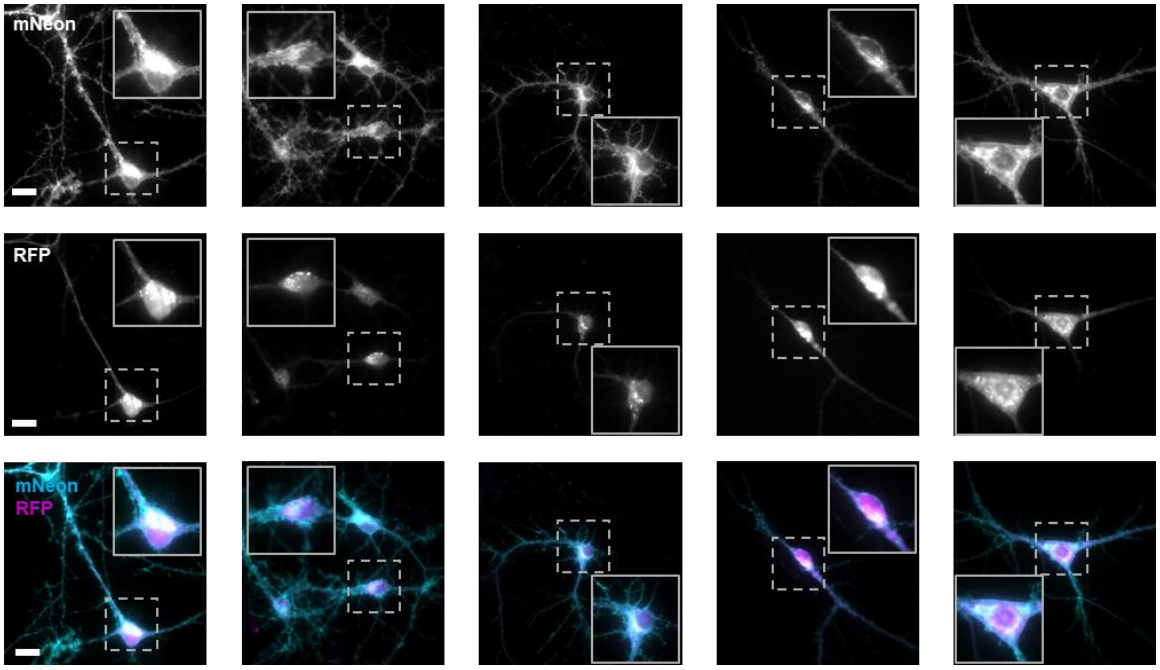


**Figure S12. Membrane trafficking of Ace2N-mNeon in neurons**. Confocal images from five randomly selected fields of view of rat hippocampal neurons co-expressing Ace2N-mNeon and a cytosolic RFP marker. Top panels: fluorescence images of Ace2N-mNeon. Middle panels: fluorescence images of RFP. Bottom panels: merged images. Scale bar = 20 μm.

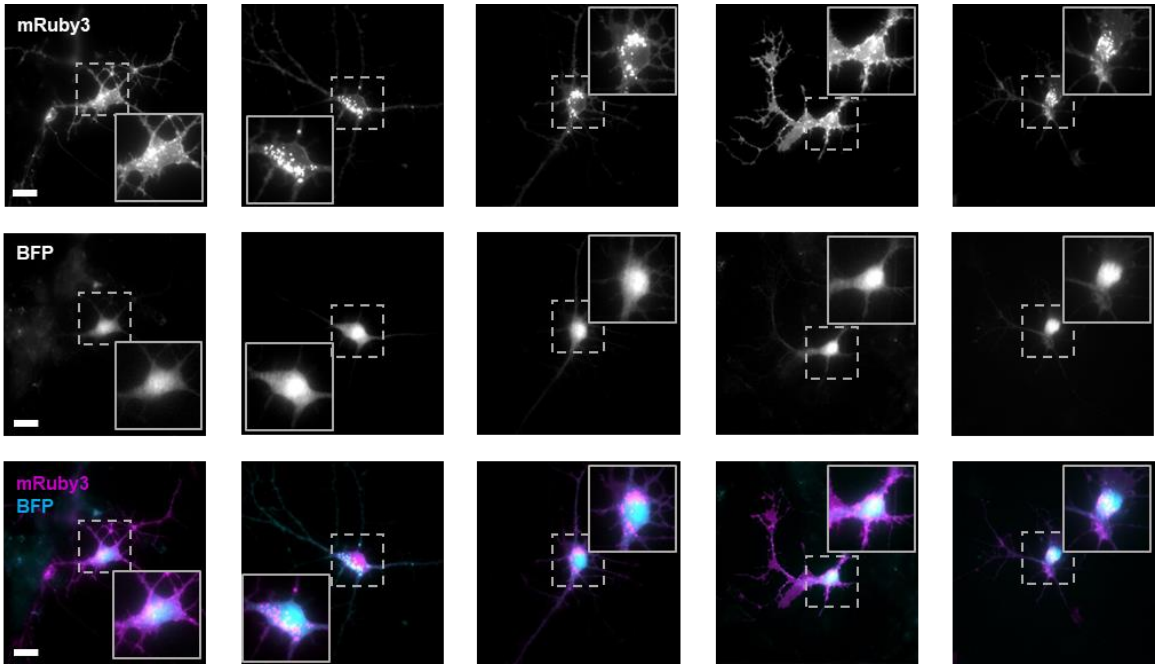


**Figure S13. Membrane trafficking of VARNAM in neurons**. Confocal images from five randomly selected fields of view of rat hippocampal neurons co-expressing VARNAM and a cytosolic BFP marker. Top panels: fluorescence images of VARNAM. Middle panels: fluorescence images of BFP. Bottom panels: merged images. Scale bar = 20 μm.

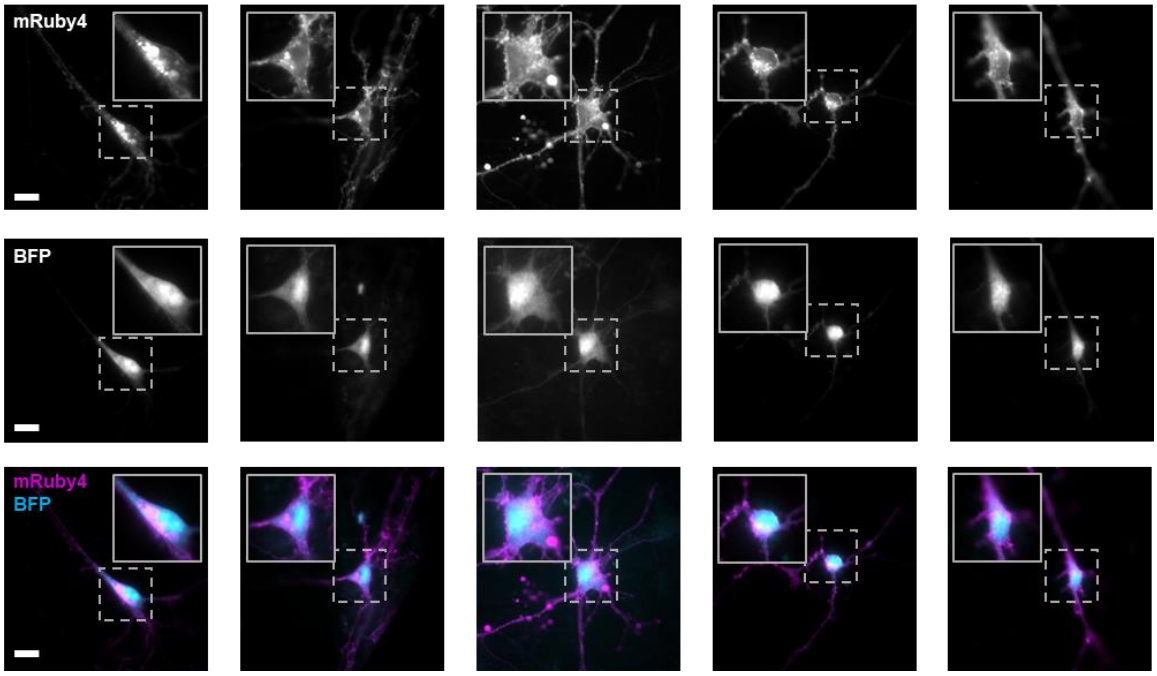


**Figure S14. Membrane trafficking of Ace(D81S)-mRuby4 in neurons**. Confocal images from five randomly selected fields of view of rat hippocampal neurons co-expressing Ace(D81S)-mRuby4 and a cytosolic BFP marker. Top panels: fluorescence images of Ace(D81S)-mRuby4. Middle panels: fluorescence images of BFP. Bottom panels: merged images. Scale bar = 20 μm.

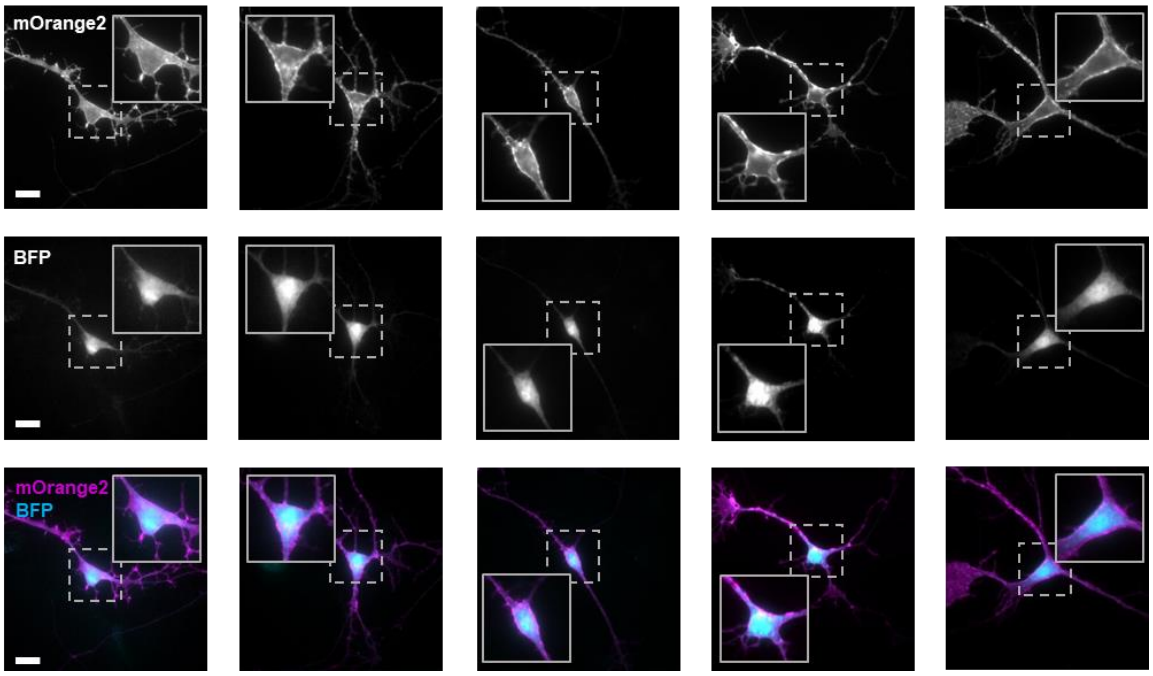


**Figure S15. Membrane trafficking of Ace(D81S)-mOrange2 in neurons**. Confocal images from five randomly selected fields of view of rat hippocampal neurons co-expressing Ace(D81S)-mOrange2 and a cytosolic BFP marker. Top panels: fluorescence images of Ace(D81S)-mOrange2. Middle panels: fluorescence images of BFP. Bottom panels: merged images. Scale bar = 20 μm.

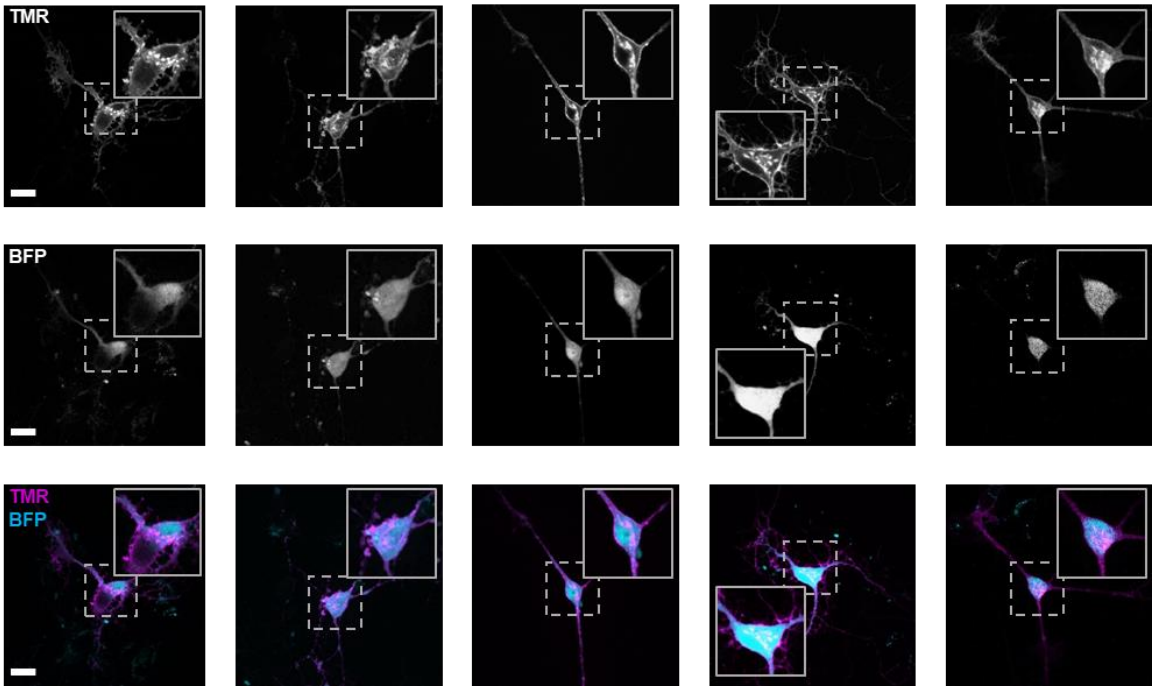


**Figure S16. Membrane trafficking of Ace(D81N)-HaloTag (Voltron) in neurons**. Confocal images from five randomly selected fields of view of rat hippocampal neurons co-expressing Ace(D81N)-HaloTag and a cytosolic BFP marker. HaloTag was labeled with a TMR-conjugated ligand. Top panels: fluorescence images of TMR. Middle panels: fluorescence images of BFP. Bottom panels: merged images. Scale bar = 20 μm.

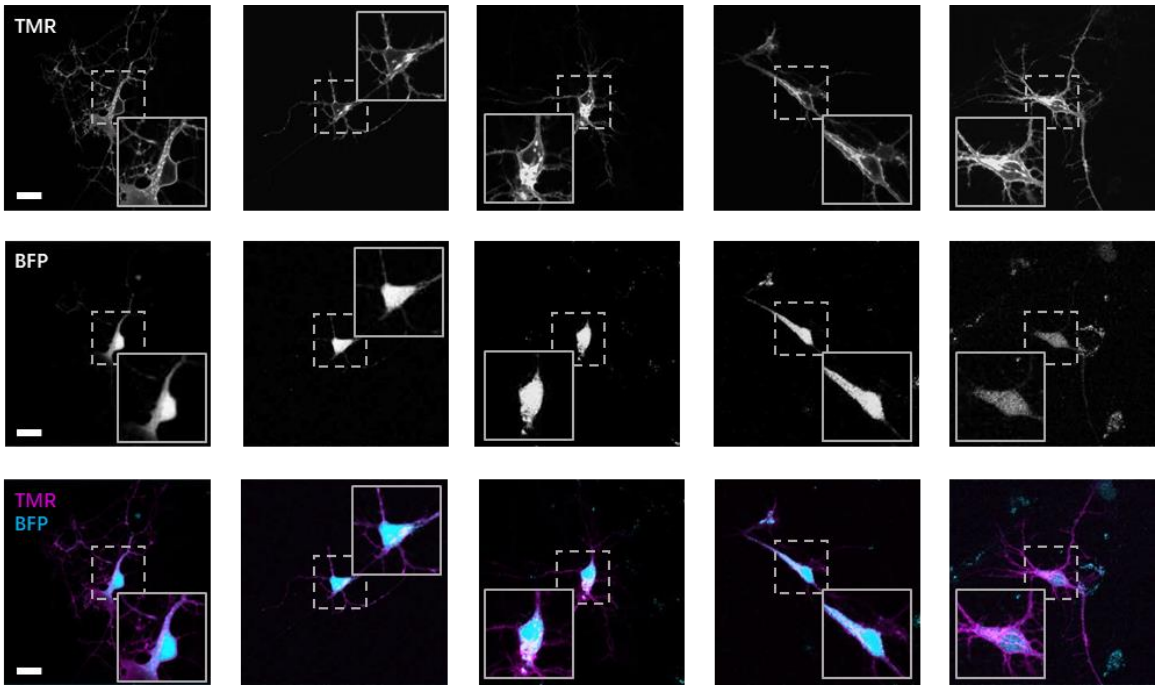


**Figure S17. Membrane trafficking of Ace(D81S)-HaloTag in neurons**. Confocal images from five randomly selected fields of view of rat hippocampal neurons co-expressing Ace(D81S)-HaloTag and a cytosolic BFP marker. HaloTag was labeled with a TMR-conjugated ligand. Top panels: fluorescence images of TMR. Middle panels: fluorescence images of BFP. Bottom panels: merged images. Scale bar = 20 μm.

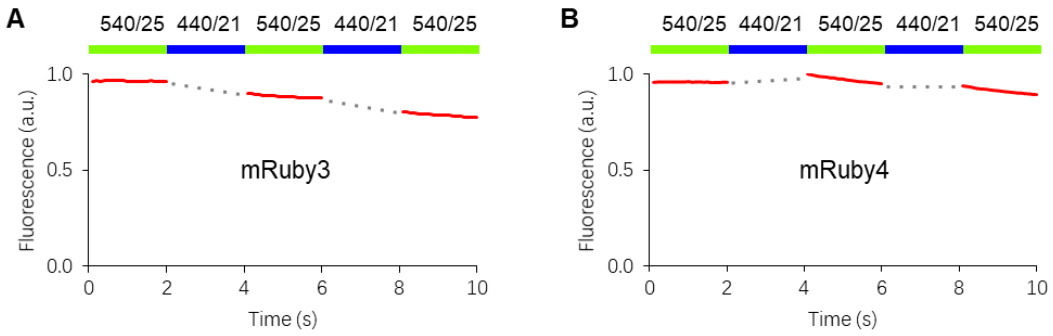


**Figure S18. Photochromic behavior of mRuby3 and mRuby4 in HEK293T cells.** HEK293T cells expressing H2B-mRuby3 (A) or H2B-mRuby4 (B) were illuminated with alternating 2-sec exposures to 540/25 nm (8.35 W/cm$^2$) and 440/21 nm (13.9 W cm$^2$) light, which has similar illumination conditions to those for mScarlet-family FPs (556/20 nm at 6.9 W/cm$^2$ and 448/20 nm at 11.5 W/cm$^2$). Note: all powers were measured close to the back-focal plane of the objective lens.

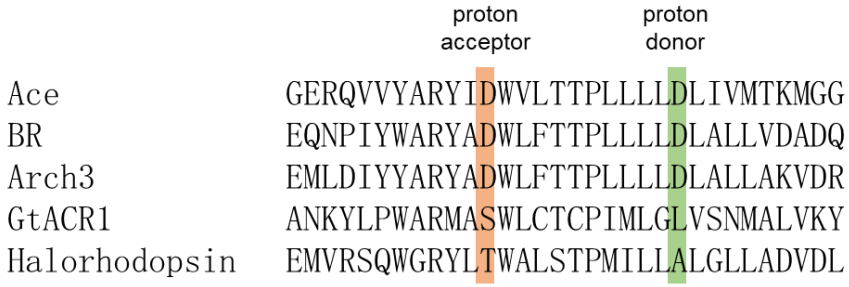


**Figure S19. Sequence alignment between rhodopsins.** Proton acceptor and donor in Ace are D81 and D92, respectively. Other rhodopsins are aligned to Ace.

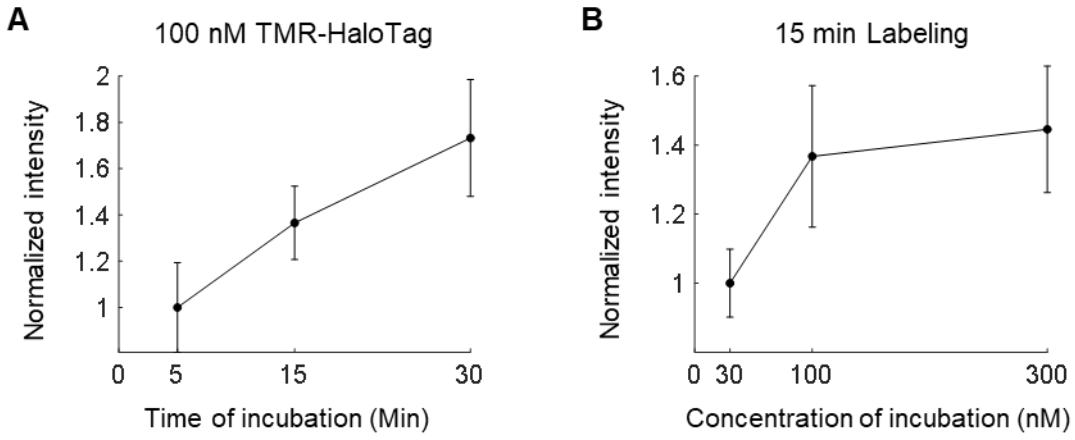


**Figure S20. Comparison of Ace(D81S)-HaloTag labeling intensities under various conditions.** (A) Normalized fluorescence intensities after 5, 15, and 30 min labeling with 100 nM TMR-HaloTag ligand. (B) Normalized fluorescence intensities after 15 min labeling with 30, 100, and 300 nM TMR-HaloTag ligand. Error bars represent s.e.m.

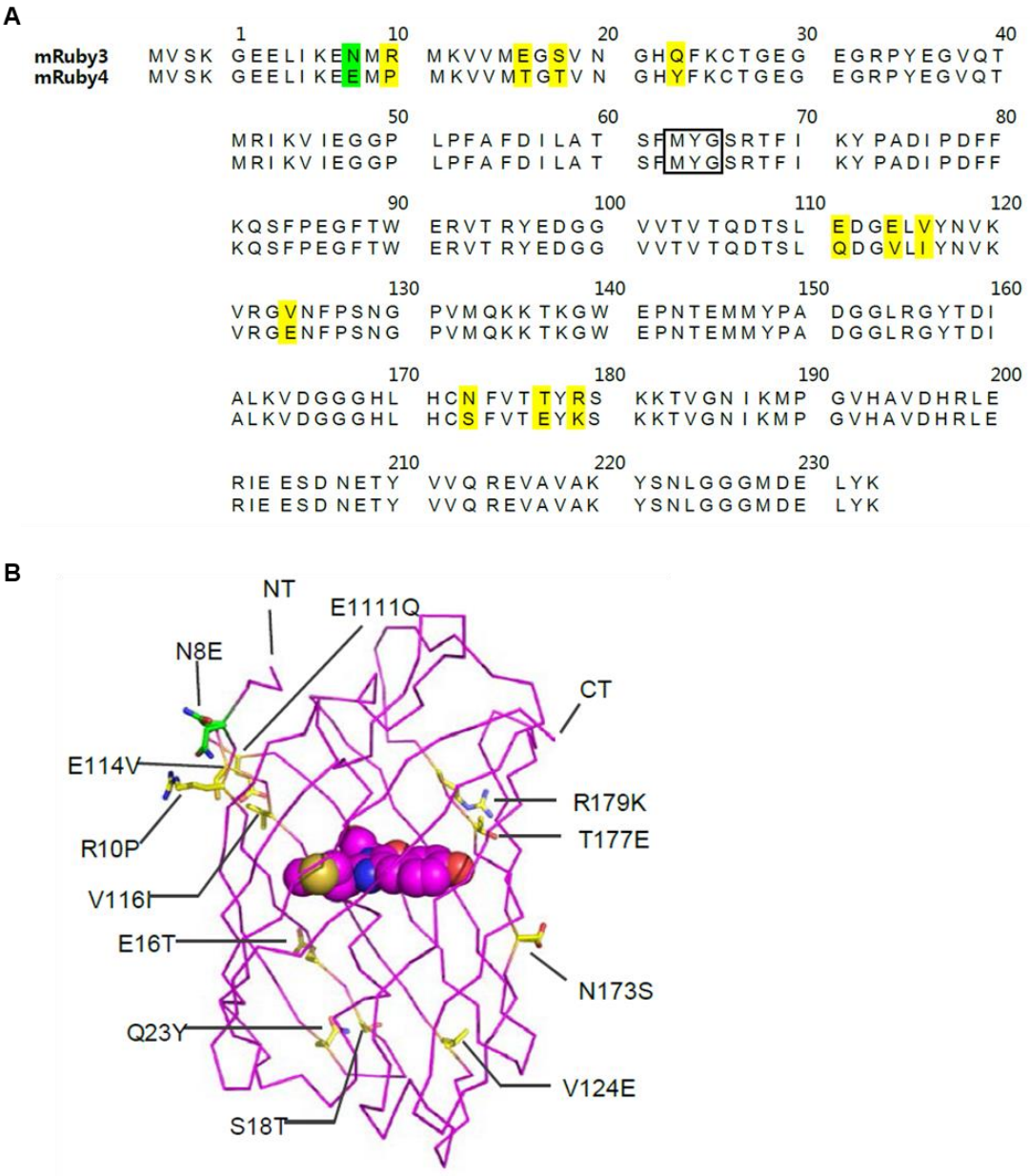


**Figure S21. mRuby4 mutations.** (A) Sequence alignment between mRuby3 and mRuby4. The amino acids forming the chromophore are indicated by a black box. Outer barrel mutations are indicated in yellow and loop mutations are indicated in green. (B) Crystal structure of mRuby (PDB accession number 3U0M) highlighting residues that are different between mRuby3 and mRuby4.

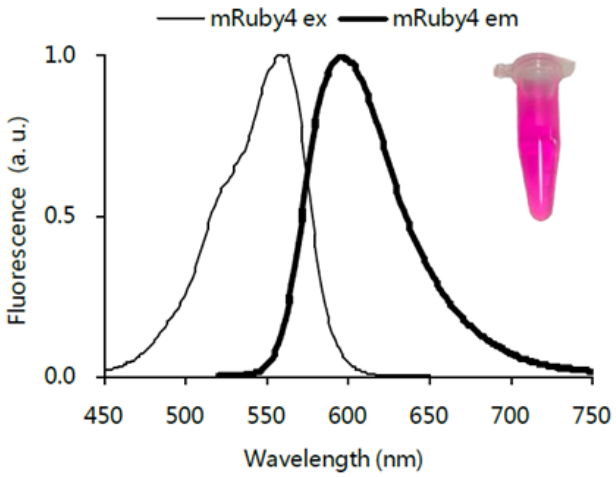


**Figure S22. Normalized excitation (left) and emission (right) spectra of mRuby4.** The inset shows the transmittance color of purified mRuby4 under room light.

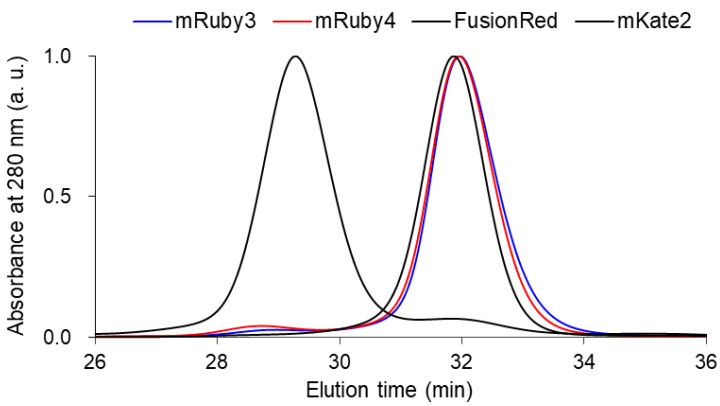


**Figure S23. Gel filtration analysis of purified fluorescent proteins.** mRuby3, mRuby4, FusionRed (monomer) and mKate2 (dimer) proteins were loaded at a concentration of 10 mg/mL.

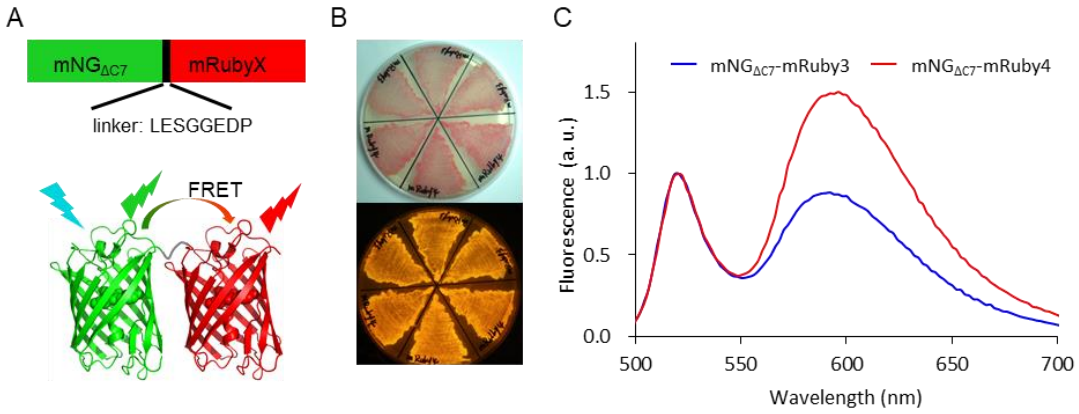


**Figure S24. FRET efficiencies of tandem fusions of CT-truncated mNeonGreen (mNG$_{\Delta C7}$, the last seven residues GMDELYK was removed) and mRubyX (X = 3 or 4).** (A) Schematic diagram of fusion constructs. (B) Bright field (top) and fluorescence images (bottom) of patches expressing fusions. All patches were kept at 4°C for 48 h after overnight cell growth at 34°C to ensure all FPs fully matured. Fluorescence images were acquired with 400- to 500-nm excitation light and a yellow acrylic long-pass filter in a Blue View Trans-illuminator (Vernier). For each panel, the upper 3 patches are mNG$_{\Delta C7}$-mRuby3 and the lower ones are mNG$_{\Delta C7}$-mRuby4. (C) FRET emission spectra of patches in (B). Fluorescence emission spectra were taken on bacteria with 450 nm excitation. The emission ratios (FRET/green) for mRuby4 and mRuby3 are 0.88 and 1.50, respectively.

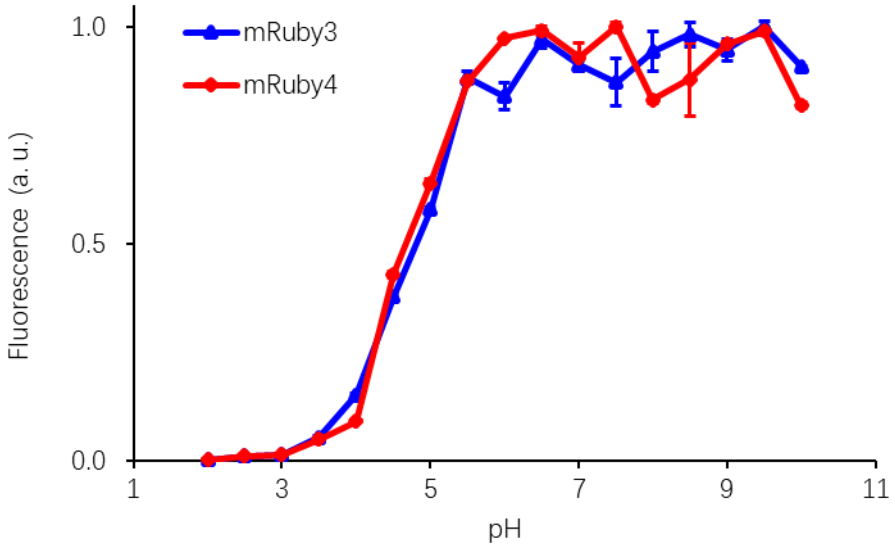


**Figure S25. pH sensitivity of mRuby variants.** Data are presented as mean ± S.D. (n=3).

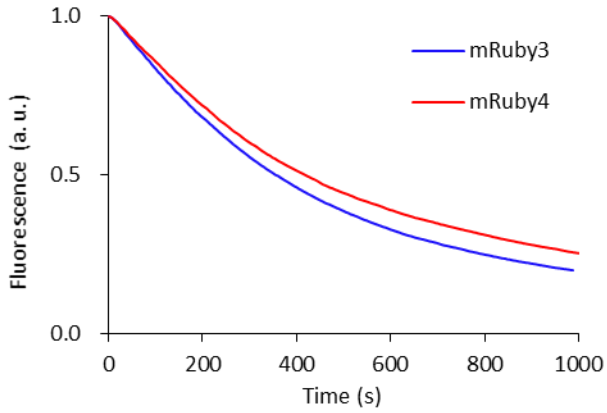


**Figure S26. Photobleaching kinetics of mRuby variants.** HEK293T cells expressing H2B-mRuby3/4 were illuminated with an arc lamp through a 540/25 nm excitation filter.

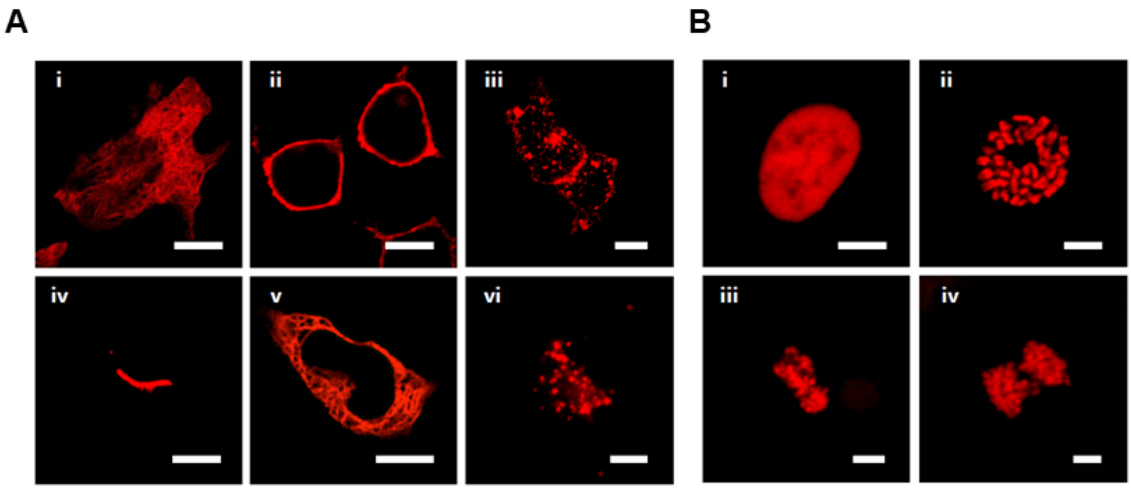


**Figure S27. Fluorescence images of HEK293T cells expressing mRuby4 fusion proteins.** (A) Images of mRuby4 fused with various organelle-targeting domains. For each fusion, the linker amino acid (aa) length is indicated between the two domains, and the origin of the fusion partner and its normal subcellular location are indicated in parentheses. i, mRuby4-18aa-tubulin (human α-tubulin, microtubules); ii, mRuby4-5aa-CAAX (human c-Ha-Ras 20-aa farnesylation signal, plasma membrane); iii, mRuby4-14aa-RhoB (human RhoB, endosomes); iv, Cx43-7aa-mRuby4 (rat α-1 connexin 43, gap junctions); v, Calnexin-14aa-mRuby4 (human calnexin sequence, endoplasmic reticulum); vi, GalT-7aa-mRuby4 (human galactosyltransferase 1, Golgi apparatus). (B) Fluorescence images of mRuby4-10aa-H2B (human histone 2B) in HEK293T cells. i, interphase; ii, prophase; iii, metaphase; iv, anaphase. Scale bar = 10 μm.

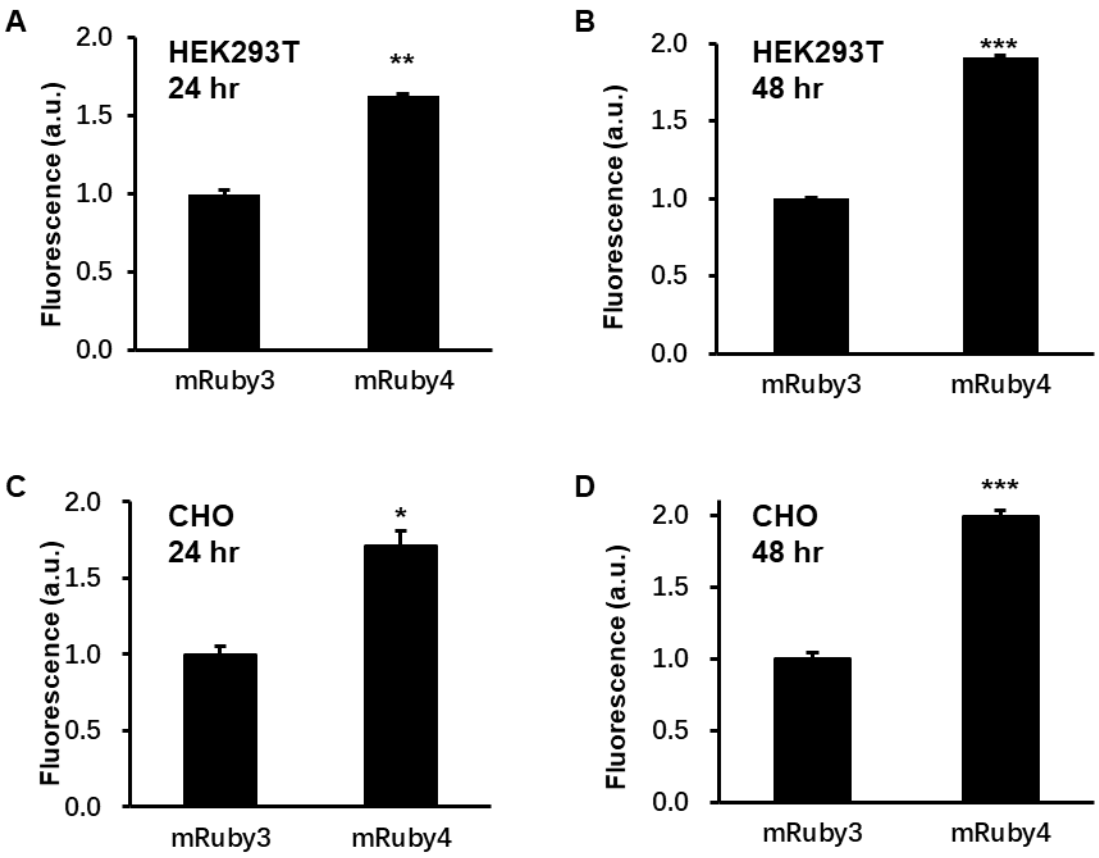


**Figure S28. Brightness comparison of mRuby3 and mRuby4 in mammalian cells.** (A-B) HEK293T cells expressing mTuoquoise2-P2A-mRuby3/4 for 24 hr (A) and 48 hr (B). (C-D) CHO cells expressing mTuoquoise2-P2A-mRuby3/4 for 24 hr (C) and 48 hr (D). The red fluorescence from mRuby4, corrected by mTuoquoise2 fluorescence, was normalized to that of mRuby3 with 1.63 at 24 hr and 1.91 at 48 hr in HEK293T cells, 1.71 at 24 hr and 1.99 at 48 hr in CHO cells. Asterisks indicate statistically significant difference (* $p < 0.05$, ** $p < 0.005$, *** $p < 0.001$). Data are presented as mean ± S.D. (n = 3).

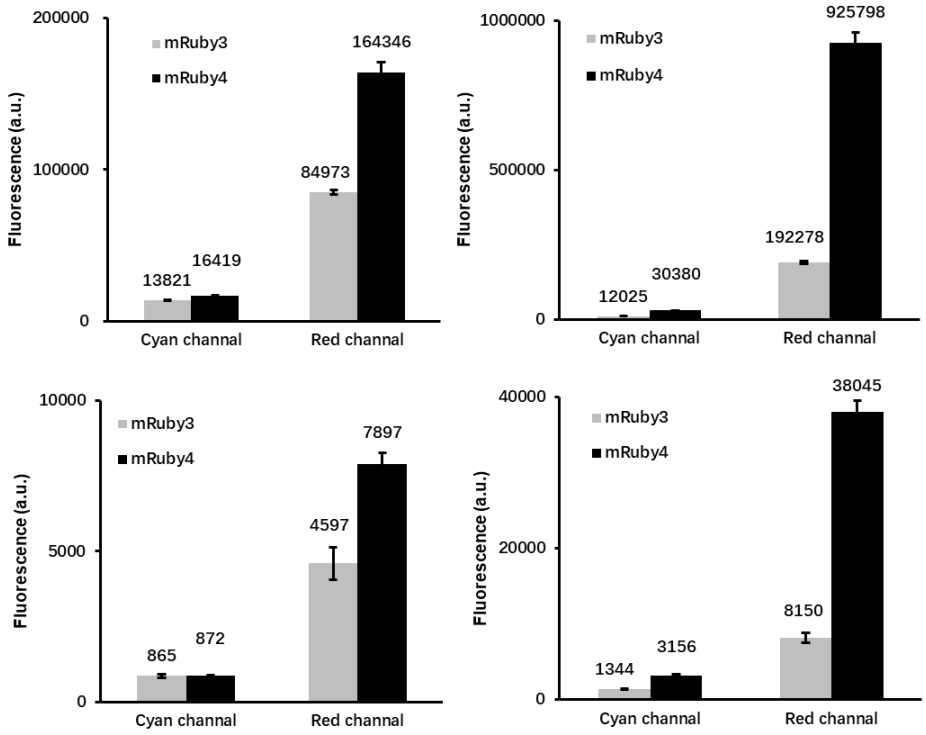


**Figure S29. Brightness comparison of mTurquoise-P2A-mRuby3/mRuby4 in both cyan and red channels.** Fluorescence signals were acquired 24 hours (left column) and 48 hours (right column) after transfection of HEK293T (top panel) and CHO cells (bottom panel). Data are presented as mean ± S.D. (n=3) and the mean values are shown right above bars.

## Supplementary Tables

**Table S1.** Properties of selected orange/red fluorescent proteins with emission peak shorter than 600 nm.

| | **mRuby4** | **mRuby3** | **mOrange2** | **mScarlet-I** | **TagRFP-T** |
|---|---|---|---|---|---|
| Excitation peak (nm) | 558 | 558 | 549 | 569 | 555 |
| Emission peak (nm) | 592 | 592 | 565 | 593 | 584 |
| EC at peak ($mM^{-1}cm^{-1}$) | 132 | 128 | 58 | 104 | 81 |
| QY | 0.45 | 0.45 | 0.6 | 0.54 | 0.41 |
| Brightness[a] | 59.6 | 57.6 | 34.8 | 56.2 | 33.2 |
| Photostability[b] | 1.18 | 1.00 | ND | ND | ND |
| pKa | 4.8 | 4.8 | 6.5 | 5.4 | 4.6 |
| Maturation efficiency[c] | 0.56 | 0.44 | ND | ND | ND |
| Oligmeric state | M | M | M | M | D |
| Reference | this work | [5] | [6] | [7] | [6] |

EC, extinction coefficient; QY, quantum yield; M, Monomer; D, Dimer; ND, not determined.

[a] Calculated as the product of EC at peak and QY.

[b] Measured in HEK293T cells and normalized to mRuby3.

[c] Functional chromophore concentration divided by total protein concentration

## Full sequences of genetic constructs used in this study

**Ace(D81S)-mOrange2**

(Blue: Signal sequence, Green: Ace, Orange: mOrange2, Purple: TS-ER2)

ATGGAGACAGACACACTCCTGCTATGGGTACTGCTGCTCTGGGTTCCAGGTTCCACTGGTG
ACTATCCATATGATGTTCCAGATTATGCTGGGGCCCAGCCGGCCAGATCTGGCCTGAACGA
CATCTTCGAGGCCCAGAAGATCGAGTGGCACGAGATGGCTGACGTGGAAACCGAGACCG
GCATGATTGCACAGTGGATTGTCTTTGCTATTATGGCTGCTGCTGCTATTGCTTTTGGAGTG
GCTGTGCACTTTCGGCCTTCAGAGCTGAAGAGCGCATACTATATCAACATTGCCATCTGCA
CTATCGCCGCTACCGCTTACTATGCAATGGCCGTGAACTACCAGGACCTGACAATGAATGG
TGAAAGGCAGGTGGTCTACGCAAGATATATTTCTTGGGTGCTGACCACACCACTGCTCCTG
CTCGATCTCATCGTCATGACCAAGATGGGCGGAGTGATGATTTCTTGGGTCATCGGCGCAG
ACATTTTCATGATCGTGTTTGGTATTCTGGGCGCCTTCGAGGATGAACACAAGTTCAAATG
GGTGTACTTTATCGCTGGATGTGTGATGCAGGCAGTCCTGACATACGGGATGTATAACGCC
ACTTGGAAAGACGATCTGAAGAAAAGCCCCGAGTACCATAGCTCCTATGTCAGTCTGCTC
GTCTTCCTGTCAATCCTCTGGGTGTTTTATCCTGTCGTGTGGGCTTTCGGGTCTGGTAGTGG
CGTGCTGTCCGTCGACAATGAGGCCATTCTCATGGGAATCCTGGATGTGCTCGCTAAGCCA
CTGTTTGGAATGGGGTGCCTCATTGCCCATGAGACTGTGAACATGGCCATCATCAAGGAGT
TCATGCGCTTCAAGGTGCGCATGGAGGGCTCCGTGAACGGCCACGAGTTCGAGATCGAGG
GCGAGGGCGAGGGCCGCCCCTACGAGGGCTTTCAGACCGCTAAGCTGAAGGTGACCAAG
GGTGGCCCCCTGCCCTTCGCCTGGGACATCCTGTCCCCTCATTTCACCTACGGCTCCAAGG
CCTACGTGAAGCACCCCGCCGACATCCCCGACTACTTCAAGCTGTCCTTCCCCGAGGGCTT
CAAGTGGGAGCGCGTGATGAACTACGAGGACGGCGGCGTGGTGACCGTGACCCAGGACT
CCTCCCTGCAGGACGGCGAGTTCATCTACAAGGTGAAGCTGCGCGGCACCAACTTCCCCT
CCGACGGCCCCGTGATGCAGAAGAAGACCATGGGCTGGGAGGCCTCCTCCGAGCGGATGT
ACCCCGAGGACGGTGCCCTGAAGGGCAAGATCAAGATGAGGCTGAAGCTGAAGGACGGC
GGCCACTACACCTCCGAGGTCAAGACCACCTACAAGGCCAAGAAGCCCGTGCAGCTGCC
CGGCGCCTACATCGTCGACATCAAGTTGGACATCACCTCCCACAACGAGGACTACACCATC
GTGGAACAGTACGAACGCGCCGAGGGCCGCCACTCCACCGGCGGCATGGACGAGCTGTA
CAAGGCTAGCAAGAGCAGAATCACCAGCGAGGGCGAGTACATCCCCCTGGACCAGATCG
ACATCAACGTGACCGGTTTCTGCTACGAGAACGAGGTGTAATGA

**Ace(D81S)-mRuby4**

(Blue: Signal sequence, Green: Ace, Red: mRuby4, Purple: TS-ER2)

ATGGAGACAGACACACTCCTGCTATGGGTACTGCTGCTCTGGGTTCCAGGTTCCACTGGTG
ACTATCCATATGATGTTCCAGATTATGCTGGGGCCCAGCCGGCCAGATCTGGCCTGAACGA
CATCTTCGAGGCCCAGAAGATCGAGTGGCACGAGATGGCTGACGTGGAAACCGAGACCG
GCATGATTGCACAGTGGATTGTCTTTGCTATTATGGCTGCTGCTGCTATTGCTTTTGGAGTG
GCTGTGCACTTTCGGCCTTCAGAGCTGAAGAGCGCATACTATATCAACATTGCCATCTGCA
CTATCGCCGCTACCGCTTACTATGCAATGGCCGTGAACTACCAGGACCTGACAATGAATGG
TGAAAGGCAGGTGGTCTACGCAAGATATATTTCTTGGGTGCTGACCACACCACTGCTCCTG
CTCGATCTCATCGTCATGACCAAGATGGGCGGAGTGATGATTTCTTGGGTCATCGGCGCAG
ACATTTTCATGATCGTGTTTGGTATTCTGGGCGCCTTCGAGGATGAACACAAGTTCAAATG
GGTGTACTTTATCGCTGGATGTGTGATGCAGGCAGTCCTGACATACGGGATGTATAACGCC
ACTTGGAAAGACGATCTGAAGAAAAGCCCCGAGTACCATAGCTCCTATGTCAGTCTGCTC
GTCTTCCTGTCAATCCTCTGGGTGTTTTATCCTGTCGTGTGGGCTTTCGGGTCTGGTAGTGG
CGTGCTGTCCGTCGACAATGAGGCCATTCTCATGGGAATCCTGGATGTGCTCGCTAAGCCA
CTGTTTGGAATGGGGTGCCTCATTGCCCATGAGACTATCTTCAAGTGGAGATCCGGACTGA
TCAAGGAAGAGATGCCCATGAAGGTGGTCATGACAGGTACCGTCAACGGCCACTACTTCA
AGTGCACAGGTGAAGGAGAAGGCAGACCGTACGAGGGAGTGCAAACCATGAGGATCAAA
GTCATCGAGGGAGGACCCCTGCCATTTGCCTTTGACATTCTTGCCACGTCGTTCATGTATGG
CAGCCGTACCTTTATCAAGTACCCGGCCGACATCCCTGATTTCTTTAAACAGTCCTTTCCTG
AGGGTTTTACTTGGGAAAGAGTTACGAGATACGAAGATGGTGGAGTCGTCACCGTCACGC
AGGACACCAGCCTTCAGGATGGCGTGCTCATCTACAACGTCAAGGTCAGAGGGGAGAACT
TTCCCTCCAATGGTCCCGTGATGCAGAAGAAGACCAAGGGTTGGGAGCCTAATACAGAGA
TGATGTATCCAGCAGATGGTGGTCTGAGAGGATACACTGACATCGCACTGAAAGTTGATGG
TGGTGGCCATCTGCACTGCAGCTTCGTGACAGAATACAAGTCAAAAAAGACCGTCGGGAA
CATCAAGATGCCCGGTGTCCATGCCGTTGATCACCGCCTGGAAAGGATCGAGGAGAGTGA
CAATGAAACCTACGTAGTGCAAAGAGAAGTGGCAGTTGCCAAATACAGCAACCTTGGTGG
TGGCATGGACGAGCTGTACAAGGCTAGCAAGAGCAGAATCACCAGCGAGGGCGAGTACA
TCCCCCTGGACCAGATCGACATCAACGTGACCGGTTTCTGCTACGAGAACGAGGTGTAAT
GA

**Ace(D81S)-Halotag**

(Green: Ace, Orange: Halotag, Purple: TS-ER2)

ATGGCTGACGTGGAAACCGAGACCGGCATGATTGCACAGTGGATTGTCTTTGCTATTATGG
CTGCTGCTGCTATTGCTTTTGGAGTGGCTGTGCACTTTCGGCCTTCAGAGCTGAAGAGCGC
ATACTATATCAACATTGCCATCTGCACTATCGCCGCTACCGCTTACTATGCAATGGCCGTGAA
CTACCAGGACCTGACAATGAATGGTGAAAGGCAGGTGGTCTACGCAAGATATATTTCCTGG
GTGCTGACCACACCACTGCTCCTGCTCGATCTCATCGTCATGACCAAGATGGGCGGAGTGA
TGATTTCTTGGGTCATCGGCGCAGACATTTTCATGATCGTGTTTGGTATTCTGGGCGCCTTC
GAGGATGAACACAAGTTCAAATGGGTGTACTTTATCGCTGGATGTGTGATGCAGGCAGTCC
TGACATACGGGATGTATAACGCCACTTGGAAAGACGATCTGAAGAAAAGCCCCGAGTACC
ATAGCTCCTATGTCAGTCTGCTCGTCTTCCTGTCAATCCTCTGGGTGTTTTATCCTGTCGTGT
GGGCTTTCGGGTCTGGTAGTGGCGTGCTGTCCGTCGACAATGAGGCCATTCTCATGGGAAT
CCTGGATGTGCTCGCTAAGCCACTGTTTGGAATGGGGTGCCTCATTGCCCATGAGACTATC
TTCAAGATCGGTACTGGCTTTCCATTCGACCCCCATTATGTGGAAGTCCTGGGCGAGCGCA
TGCACTACGTCGATGTTGGTCCGCGCGATGGCACCCCTGTGCTGTTCCTGCACGGTAACCC
GACCTCCTCCTACGTGTGGCGCAACATCATCCCGCATGTTGCACCGACCCATCGCTGCATT
GCTCCAGACCTGATCGGTATGGGCAAATCCGACAAACCAGACCTGGGTTATTTCTTCGACG
ACCACGTCCGCTTCATGGATGCCTTCATCGAAGCCCTGGGTCTGGAAGAGGTCGTCCTGGT
CATTCACGACTGGGGCTCCGCTCTGGGTTTCCACTGGGCCAAGCGCAATCCAGAGCGCGT
CAAAGGTATTGCATTTATGGAGTTCATCCGCCCTATCCCGACCTGGGACGAATGGCCAGAA
TTTGCCCGCGAGACCTTCCAGGCCTTCCGCACCACCGACGTCGGCCGCAAGCTGATCATC
GATCAGAACGTTTTTATCGAGGGTACGCTGCCGATGGGTGTCGTCCGCCCGCTGACTGAAG
TCGAGATGGACCATTACCGCGAGCCGTTCCTGAATCCTGTTGACCGCGAGCCACTGTGGC
GCTTCCCAAACGAGCTGCCAATCGCCGGTGAGCCAGCGAACATCGTCGCGCTGGTCGAAG
AATACATGGACTGGCTGCACCAGTCCCCTGTCCCGAAGCTGCTGTTCTGGGGCACCCCAG
GCGTTCTGATCCCACCGGCCGAAGCCGCTCGCCTGGCCAAAAGCCTGCCTAACTGCAAGG
CTGTGGACATCGGCCCGGGTCTGAATCTGCTGCAAGAAGACAACCCGGACCTGATCGGCA
GCGAGATCGCGCGCTGGCTGTCGACGCTCGAGATTTCCGGCGAGCCAACCACTAAGAGCA
GAATCACCAGCGAGGGCGAGTACATCCCCCTGGACCAGATCGACATCAACGTGTTCTGCT
ACGAGAACGAGGTG

**Ace(D81S)-SNAP-tag**

(Green: Ace, Orange: SNAP-tag, Blue: Flag tag, Purple: TS-ER2)

ATGGCTGACGTGGAAACCGAGACCGGCATGATTGCACAGTGGATTGTCTTTGCTATTATGG
CTGCTGCTGCTATTGCTTTTGGAGTGGCTGTGCACTTTCGGCCTTCAGAGCTGAAGAGCGC
ATACTATATCAACATTGCCATCTGCACTATCGCCGCTACCGCTTACTATGCAATGGCCGTGAA
CTACCAGGACCTGACAATGAATGGTGAAAGGCAGGTGGTCTACGCAAGATATATTTCCTGG
GTGCTGACCACACCACTGCTCCTGCTCGATCTCATCGTCATGACCAAGATGGGCGGAGTGA
TGATTTCTTGGGTCATCGGCGCAGACATTTTCATGATCGTGTTTGGTATTCTGGGCGCCTTC
GAGGATGAACACAAGTTCAAATGGGTGTACTTTATCGCTGGATGTGTGATGCAGGCAGTCC
TGACATACGGGATGTATAACGCCACTTGGAAAGACGATCTGAAGAAAAGCCCCGAGTACC
ATAGCTCCTATGTCAGTCTGCTCGTCTTCCTGTCAATCCTCTGGGTGTTTTATCCTGTCGTGT
GGGCTTTCGGGTCTGGTAGTGGCGTGCTGTCCGTCGACAATGAGGCCATTCTCATGGGAAT
CCTGGATGTGCTCGCTAAGCCACTGTTTGGAATGGGGTGCCTCATTGCCCATGAGACTATC
TTCAAGAAGATGTCCGGAATGGACAAAGATTGCGAAATGAAACGTACCACCCTGGATAGC
CCGCTGGGCAAACTGGAACTGAGCGGCTGCGAACAGGGCCTGCATGAAATTAAACTGCTG
GGTAAAGGCACCAGCGCGGCCGATGCGGTTGAAGTTCCGGCCCCGGCCGCCGTGCTGGGT
GGTCCGGAACCGCTGATGCAGGCGACCGCGTGGCTGAACGCGTATTTTCATCAGCCGGAA
GCGATTGAAGAATTTCCGGTTCCGGCGCTGCATCATCCGGTGTTTCAGCAGGAGAGCTTTA
CCCGTCAGGTGCTGTGGAAACTGCTGAAAGTGGTTAAATTTGGCGAAGTGATTAGCTATCA
GCAGCTGGCGGCCCTGGCGGGTAATCCGGCGGCCACCGCCGCCGTTAAAACCGCGCTGAG
CGGTAACCCGGTGCCGATTCTGATTCCGTGCCATCGTGTGGTTAGCTCTAGCGGTGCGGTT
GGCGGTTATGAAGGTGGTCTGGCGGTGAAAGAGTGGCTGCTGGCCCATGAAGGTCATCGT
CTGGGTAAACCGGGTCTGGGAGATTACAAGGATGACGACGATAAGAAGAAGAGCAGGAT
CACCAGCGAGGGCGAGTACATCCCCCTGGACCAGATCGACATCAACGTGTTCTGCTACGA
GAACGAGGTG

# References


1. Xu, Y.; Peng, L.; Wang, S.; Wang, A.; Ma, R.; Zhou, Y.; Yang, J.; Sun, D. E.; Lin, W.; Chen, X.; Zou, P., Hybrid Indicators for Fast and Sensitive Voltage Imaging. *Angew Chem Int Ed Engl* **2018,***57* (15), 3949-3953.
2. Gibson, D. G., Enzymatic assembly of overlapping DNA fragments. *Methods Enzymol* **2011,***498*, 349-61.
3. Chu, J.; Oh, Y.; Sens, A.; Ataie, N.; Dana, H.; Macklin, J. J.; Laviv, T.; Welf, E. S.; Dean, K. M.; Zhang, F.; Kim, B. B.; Tang, C. T.; Hu, M.; Baird, M. A.; Davidson, M. W.; Kay, M. A.; Fiolka, R.; Yasuda, R.; Kim, D. S.; Ng, H. L.; Lin, M. Z., A bright cyan-excitable orange fluorescent protein facilitates dual-emission microscopy and enhances bioluminescence imaging in vivo. *Nat Biotechnol* **2016,***34* (7), 760-7.
4. Gross, L. A.; Baird, G. S.; Hoffman, R. C.; Baldridge, K. K.; Tsien, R. Y., The structure of the chromophore within DsRed, a red fluorescent protein from coral. *Proc Natl Acad Sci U S A* **2000,***97* (22), 11990-5.
5. Bajar, B. T.; Wang, E. S.; Lam, A. J.; Kim, B. B.; Jacobs, C. L.; Howe, E. S.; Davidson, M. W.; Lin, M. Z.; Chu, J., Improving brightness and photostability of green and red fluorescent proteins for live cell imaging and FRET reporting. *Sci Rep* **2016,***6*, 20889.
6. Shaner, N. C.; Lin, M. Z.; McKeown, M. R.; Steinbach, P. A.; Hazelwood, K. L.; Davidson, M. W.; Tsien, R. Y., Improving the photostability of bright monomeric orange and red fluorescent proteins. *Nat Methods* **2008,***5* (6), 545-51.
7. Bindels, D. S.; Haarbosch, L.; van Weeren, L.; Postma, M.; Wiese, K. E.; Mastop, M.; Aumonier, S.; Gotthard, G.; Royant, A.; Hink, M. A.; Gadella, T. W., Jr., mScarlet: a bright monomeric red fluorescent protein for cellular imaging. *Nat Methods* **2017,***14* (1), 53-56.